

Theoretical comparison of optical and electronic properties of uniformly and randomly arranged nano-porous ultra-thin layers

Aliaksandr Hubarevich,¹ Mikita Marus,¹ Weijun Fan,¹ Aliaksandr Smirnov,²
Xiao Wei Sun,^{1,3} and Hong Wang^{1,*}

¹*School of Electrical and Electronic Engineering, Nanyang Technological University, 50 Nanyang Avenue, 639798, Singapore*

²*Department of Micro- and Nano-Electronics, Belarusian State University of Informatics and Radioelectronics, 6 P. Brovki, Minsk, 220013, Belarus*

³*EXWSUN@ntu.edu.sg*

**EWANGHONG@ntu.edu.sg*

Abstract: The theoretical comparison of optical and electronic properties of *aluminum* and *silver* nano-porous ultra-thin layers in terms of the arrangement and size of the pores was presented. The uniform nano-porous layers exhibit a slightly higher average transmittance (up to 10%) in the wavelength range of the plasmonic response in comparison to the randomly arranged ones. Compared to uniform nano-porous layers, a much larger sheet resistance (up to 12 times) for random nano-porous layers is observed. The uniform and random *Ag* nano-porous layers possessing the strong plasmonic response over whole visible range can reach an average transmittance of 90 and 80% at the sheet resistance of 10 and 20 Ohm/sq, respectively, which is comparable to widely used ITO electrodes.

©2015 Optical Society of America

OCIS codes: (130.0250) Optoelectronics; (310.7005) Transparent conductive coatings; (240.6680) Surface plasmons.

References and links

1. M.-G. Kang and L. J. Guo, "Metal transfer assisted nanolithography on rigid and flexible substrates," *J. Vac. Sci. Technol. B* **26**(6), 2421–2425 (2008).
2. M. G. Kang, M. S. Kim, J. Kim, and L. J. Guo, "Organic solar cells using nanoimprinted transparent metal electrodes," *Adv. Mater.* **20**(23), 4408–4413 (2008).
3. J. van de Groep, P. Spinelli, and A. Polman, "Transparent conducting silver nanowire networks," *Nano Lett.* **12**(6), 3138–3144 (2012).
4. P. B. Catrysse and S. Fan, "Nanopatterned metallic films for use as transparent conductive electrodes in optoelectronic devices," *Nano Lett.* **10**(8), 2944–2949 (2010).
5. Q. G. Du, K. Sathiyamoorthy, L. P. Zhang, H. V. Demir, C. H. Kam, and X. W. Sun, "A two-dimensional nanopatterned thin metallic transparent conductor with high transparency from the ultraviolet to the infrared," *Appl. Phys. Lett.* **101**(18), 181112 (2012).
6. H. Wu, L. Hu, M. W. Rowell, D. Kong, J. J. Cha, J. R. McDonough, J. Zhu, Y. Yang, M. D. McGehee, and Y. Cui, "Electrospun metal nanofiber webs as high-performance transparent electrode," *Nano Lett.* **10**(10), 4242–4248 (2010).
7. P. Kuang, J. M. Park, W. Leung, R. C. Mahadevapuram, K. S. Nalwa, T. G. Kim, S. Chaudhary, K. M. Ho, and K. Constant, "A new architecture for transparent electrodes: relieving the trade-off between electrical conductivity and optical transmittance," *Adv. Mater.* **23**(21), 2469–2473 (2011).
8. M. Marus, A. Hubarevich, H. Wang, A. Smirnov, X. Sun, and W. Fan, "Optoelectronic performance optimization for transparent conductive layers based on randomly arranged silver nanorods," *Opt. Express* **23**(5), 6209–6214 (2015).
9. P.-C. Hsieh, C.-J. Chung, J. McMillan, M.-A. Tsai, M. Lu, N. Panoiu, and C. W. Wong, "Photon transport enhanced by transverse Anderson localization in disordered superlattices," *Nat. Phys.* **11**(3), 268–274 (2015).
10. M. Rycenga, C. M. Cobley, J. Zeng, W. Li, C. H. Moran, Q. Zhang, D. Qin, and Y. Xia, "Controlling the synthesis and assembly of silver nanostructures for plasmonic applications," *Chem. Rev.* **111**(6), 3669–3712 (2011).
11. Lumerical FDTD Solutions, <https://www.lumerical.com/tcad-products/fdtd/>.

12. M. Weber and M. R. Kamal, "Estimation of the volume resistivity of electrically conductive composites," *Polym. Compos.* **18**(6), 711–725 (1997).
13. B. Last and D. Thouless, "Percolation theory and electrical conductivity," *Phys. Rev. Lett.* **27**(25), 1719–1721 (1971).
14. A. Smirnov, A. Stsiapanau, A. Mohammed, E. Mukha, H. Kwok, and A. Murauski, "Combined nanostructured layers for display applications," in *SID Symposium "Display Week-2011"* (Wiley Online Library, 2011), pp. 1385–1387.
15. B. Huttner, "Optical properties of polyvalent metals in the solid and liquid state: aluminium," *J. Phys. Condens. Matter* **6**(13), 2459–2474 (1994).

1. Introduction

Metallic nano-patterned layers are potential candidates for being used as transparent conductive electrodes [1–7]. Transmittance of around 80 to 90% and sheet resistance ranging from 10 to 50 Ohm/sq can be realized by nano-patterned metallic layers, which are comparable to the most common transparent conductive layers (TCLs), such as the indium tin oxide (ITO). Aluminum (*Al*), gold (*Au*), copper (*Cu*), platinum (*Pt*) and silver (*Ag*) were commonly used for the nano-patterned TCLs [1–5]. However, the specific influence of the wavelength of the plasmonic response on the optical performance of the metallic TCLs remains a problem. Another important issue is connected with nano-pattern arrangement. So far, TCLs with both uniformly and randomly arranged patterns are experimentally demonstrated [8, 9]. However, the impact of nano-pattern arrangement on the optical and the electronic properties remains unexplored.

This paper presents a detailed theoretical study of the influence of the uniform and random porous *Al* and *Ag* layers on the opto-electrical properties in the visible range from 400 to 750 nm. It is found that the electrical properties of the nano-porous layers could be largely affected by the ordering of the pores. Much lower sheet resistance can be achieved if the nano-pores are ordered. In the meantime, the optical properties are mainly affected by the arrangement of the pores in the wavelength range of the plasmonic response, which is below 600 and from 300 to 1200 nm for *Al*- and *Ag-air* interface respectively [10].

2. Methodology

Nano-porous metallic layers of *Al* and *Ag* on a glass substrates with an area of $2 \times 2 \mu\text{m}$ size were used in the simulations. Full depth pores of cylindrical shape were aligned parallel to *Z* axis as shown in Fig. 1. Each specific pore location was determined according to $(a + da)_i$, where a is the i^{th} pore initial position in the hexagonal arrangement and da is the i^{th} pore deviation along *XY* plane. Each pore radius was obtained by adding of the deviated value dr to the initial radius r : $(r + dr)_i$. The normal distribution was used to get da and dr to create non-uniform porous layers. Four cases were examined: (a) the layer with constant pore radius and interpore distance; (b) the layer with random pore radius and constant interpore distance; (c) the layer with constant pore radius and random interpore distance; and (d) the layer with random pore radius and interpore distance [see Figs. 1(a)-1(d) accordingly].

The optical properties were simulated using the finite-difference time-domain method (FDTD) which is commercially available from the Lumerical software [11]. The incident light was distributed along *Z* axis. The periodic boundary conditions and the perfectly matched layers were applied parallel and perpendicular to *Z* axis correspondingly. The mesh size of the metallic layer was set to 5, 5 and 2.5 nm in *X*, *Y*, and *Z* axes respectively.

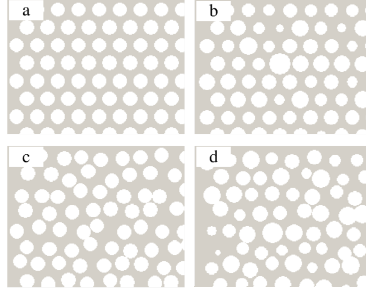


Fig. 1. Geometrical model for the distribution of the uniformly and the randomly arranged nano-porous layers. Layer types: (a) constant pore radius and inter-pore distance; (b) random pore radius and constant inter-pore distance; (c) constant pore radius and random inter-pore distance; (d) random pore radius and inter-pore distance.

The sheet resistance was calculated using the percolation model [12, 13], which is given by:

$$R_{sh} = \frac{1}{h\sigma_0(\phi_f - \phi_{crit})^t}, \quad (1)$$

where R_{sh} , h , σ_0 , ϕ_f , ϕ_{crit} and t are the sheet resistance, the layer thickness, the bulk layer conductivity, the nano-patterned metal volume fraction, the critical nano-patterned metal volume fraction when the conductivity is tending to zero and the critical exponent, respectively. The value of t was set to 1.1 for 2D structure according to earlier study [12].

3. Results and discussion

The nano-porous layer thickness h and the inter-pore distance a were chosen as 10 and 100 nm, respectively [5]. The ratio of the pore radius to the inter-pore distance r/a was varied from 0 to 0.5 for the uniform pore arrangement, i.e. from no pores (the bulk material) to their connection with each other (when the conductivity is approaching to zero). According to the experimental data from [13], the above-mentioned interval of r/a for the randomly arranged nano-porous layer can range from 0 to 0.4. Therefore, the r/a value has to be equal or less than 0.4 to keep the metal volume comparable for both uniform and random porous layers to ensure that pores cannot be overlapped. Considering the deviation of the pore radius and the inter-pore distance, the condition of $r/a \leq 0.4$ is transformed into the equation given below:

$$\frac{(r + dr)_i}{(a + da)_i} \leq 0.4. \quad (2)$$

The deviation of the pore radius dr and pore radius r were chosen in agreement with the experimental data reported by A. Smirnov et. al. [14]: dr can be varied from 0 up to 20%, while r was set to 33 nm. The parameters dr and r were set to fulfill the Eq. (2) as shown in Table 1. Layer types *A*, *B*, *C* and *D* are related to the pore arrangement shown in Figs. 1(a)-1(d), respectively.

Figure 2 presents the transmittance, the reflectance and the absorbance of the *Al* nano-porous layer for the four cases according to Table 1. As we can see, the highest transmittance is observed for the uniformly arranged layer (case *A*). The reduction in transmittance in the spectrum range from 650 to 850 nm is due to the inter-band electron transition [15]. The transformation of the pore radius from ordered to random (case *B*) causes a decrease in the average transmittance around 5% in the wavelength range from 300 to 600 nm. The disordering of the pore position (case *C*) results in a continuous reduction of transmittance in the same wavelength range up to 10%. The largest difference of the transmittance between

the uniform and the random pore layers is observed for the case *D* and is 12%. Such behavior is caused by the change of the reflectance and the absorbance [Figs. 2(b) and 2(c)]. It should

Table 1. Deviation of the pore radius and interpore distance of the nano-porous layers.

Layer type	Deviation of the pore radius dr (nm)	Deviation of the interpore distance da (nm)
<i>A</i>	0	0
<i>B</i>	(0, 6)	0
<i>C</i>	0	(0, 10)
<i>D</i>	(0, 6)	(0, 10)

Note: (μ, σ) is the normal distribution with the mean μ and the standard deviation σ .

be mentioned that the absorbance is increasing for *B*, *C* and *D* layers along the whole wavelength range. The reflectance shows the similar behavior in the wavelength range of the plasmonic response from 300 to 500 nm, while the contrary effect is observed in the wavelength range from 500 to 900 nm. These effects can be explained under the framework of localization of waves, which increases absorbance by the interband electron transition and decrease reflectance in *Al* in the range of 500-900 nm. The contrary effect of reflectance from 300 to 500 nm can be attributed to the plasmonic response of *Al*. Therefore, it is necessary to further investigate *Ag* nano-porous layer possessing strong plasmonic response over the whole simulation wavelength range [8].

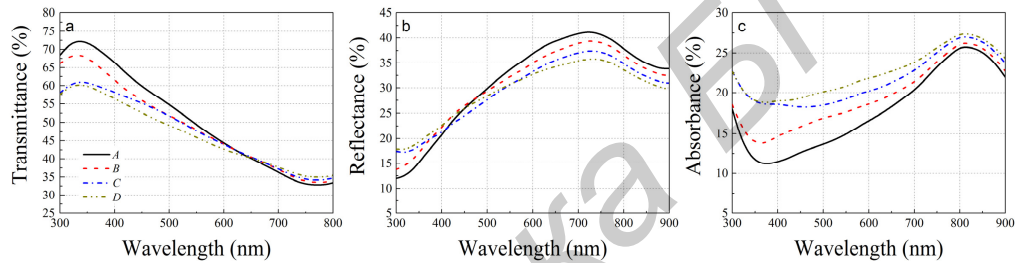


Fig. 2. The dependence of the optical properties on the wavelength of *Al* nano-porous layer. The curve names are related to the layer types *A-D* from Table 1.

Figure 3 shows the transmittance, the reflectance and the absorbance of *Ag* nano-porous layer for the four cases in accordance with Table 1. The dropping of the transmittance for *Ag* layers covers broader wavelength range in comparison to *Al* ones. The transformation of the radius of pores from ordered to random (case *B*) results in the 5-7% decrease of the transmittance over the range from 400 to 900 nm. The disordering of pore position (case *C*) provokes the transmittance dropping of 7-10% in the same wavelength range. The largest difference of the transmittance is for the case *D*, which is 10-12%. The changing of the transmittance for the above mentioned cases is accompanied by the increasing of both reflectance and absorbance in the corresponding wavelength range [see Figs. 3(b) and 3(c)]. It can be seen, higher disordering of the pore radius as well as interpore distance results in larger increment of the reflectance and the absorbance. This phenomena is illustrated in Fig. 4, where the electric field intensity distribution is shown for the cases *A* and *B*. The uniformly arranged layer has the distribution of the electric field intensity directed straightly along the propagation of the electric field *E* [Fig. 4(a)]. However, the randomly arranged layer has many definite areas with higher localization of the electric field intensity [Fig. 4(b)]. The plasmonic response characterized by the coupling of incoming photons and free electrons in a metal may provoke two types of interaction. One is called the localized surface plasmons

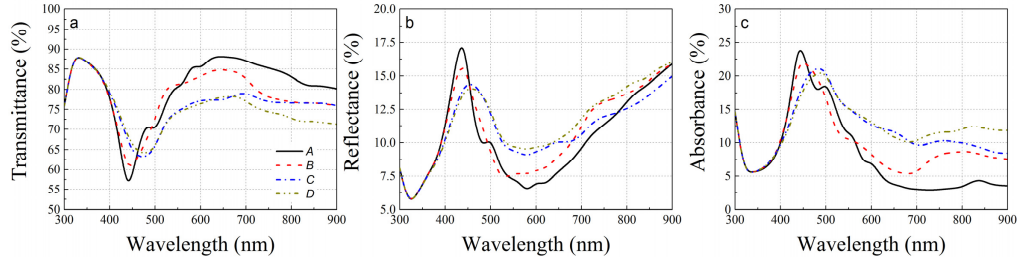


Fig. 3. The dependence of the optical properties on the wavelength of Ag nano-porous layer. The curve names are related to the layer types A-D from Table 1.

(LSPs), where the metallic nano-patterns are optically isolated from each other. Another type is the surface plasmon polaritons (SPPs), where the nano-patterns are optically close to each other, which permits electromagnetic waves propagation along the nano-patterns. Therefore, the nano-porous layers can exhibit either LSPs or SPPs or both types of the photon-electron interaction depending on the nano-pore size, arrangement and inter-pore distance. It is obvious, that SPPs are prevailing within the uniformly arranged layers. The pores disordering effect causes reduction of the SPPs propagation length, which leads to the intensification of the LSPs. Therefore, the localization of light creates many optically isolated nano-pattern areas possessing LSPs, which, in turn, induces the higher reflectance and the absorbance in the corresponding range of the plasmonic response.

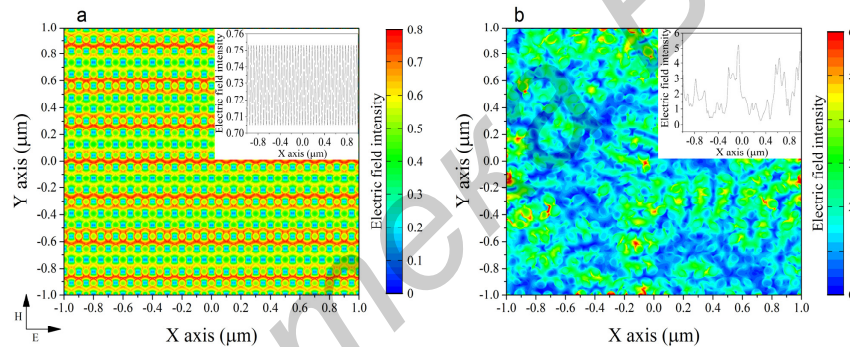


Fig. 4. Electric field intensity distribution of ordered (a) and random (b) nano-porous Ag layers at 600 nm wavelength. XY plane is located at the center of the metal layer thickness. Insertions show the electric field intensity distribution at $Y = 0$.

Figures 5(a) and 5(c) show the average transmittance against the ratio of the pore radius to the inter-pore distance r/a in the range from 400 to 750 nm for the uniformly and the randomly arranged nano-porous Al and Ag layers. As can be seen the transmittance of the uniform Al nano-porous layer varies from 15 to 85% when r/a increases from 0 to 0.48, while the transmittance of the random one varies from 15 to 58% with increment of r/a from 0 to 0.4. The maximum transmittance for the uniformly and the randomly arranged Al conductive nano-porous layers is around 85 and 60% respectively. The discrepancy of the transmittance becomes noticeable from r/a around 0.15 and reaches the maximum of 10% at r/a around 0.4. A larger discrepancy is observed in case of the nano-porous Ag layer. The transmittance of the uniform Ag nano-porous layer varies from 63 to 94% when r/a increases from 0 to 0.48, while the transmittance of the random one varies from 63 to 80% with increment of r/a from 0 to 0.4. The discrepancy of the transmittance for the uniformly and randomly arranged Ag nano-porous layers starts to be seen when r/a is larger than 0.11 and reaches its maximum of 7% at r/a around 0.4. Overall, we can conclude that the nano-thin layers of the materials possessing the plasmonic response in the investigated wavelength range demonstrate higher optical performance for both uniformly and randomly arranged nano-porous structures.

Figures 5(b) and 5(d) show the sheet resistance against ratio of the pore radius to the inter-pore distance r/a for the uniformly and the randomly arranged nano-porous *Al* and *Ag* layers. According to the percolation theory [12, 13], the critical nano-porous metal volume fraction ϕ_{crit} is the key value affecting the sheet resistance for both the uniform and the random nano-porous layers. The sheet resistance of the uniform *Al* nano-porous layer varies from 2 to 55 Ohm/sq when r/a increases from 0 to 0.48, while the sheet resistance of the random one drastically increases from 2 to 700 Ohm/sq with the increment of r/a from 0 to 0.4. The sheet resistance of *Ag* nano-porous layer is 1.8 times smaller in comparison to *Al* one caused by the distinction of their bulk conductivity σ_0 : 6.3×10^7 (*Ag*) and 3.5×10^7 (*Al*) S/m.

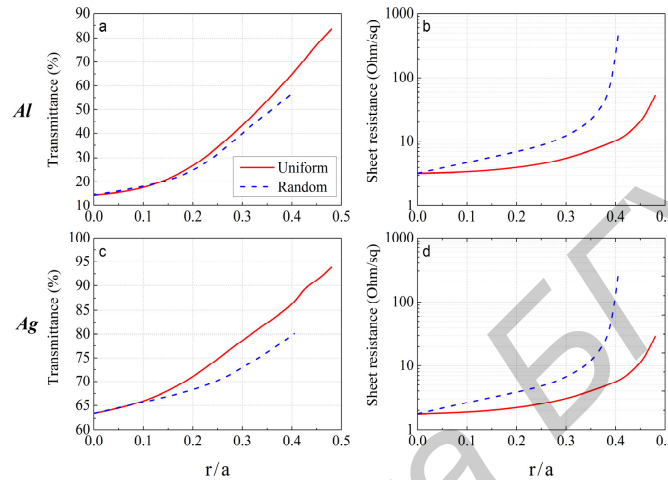


Fig. 5. The dependence of the average transmittance (a, c) and the sheet resistance (b, d) on the ratio of the pore radius to the inter-pore distance r/a for the uniformly and the randomly arranged nano-porous *Al* and *Ag* layers in the range from 400 to 750 nm.

Considering the optical and the electronic properties in terms of the TCL applications (Fig. 5), it can be seen that uniformly arranged *Al* nano-porous layer possess the transmittance of 80% at the sheet resistance of 25 Ohm/sq, while the randomly arranged one has only 50% transmittance at the same sheet resistance. However, different situation is observed for *Ag*: the uniform nano-porous layers possess transmittance around 90% at 10 Ohm/sq, while the random ones reach only 80% transmittance with higher sheet resistance of 20 Ohm/sq.

4. Conclusion

The modification of the optical and the electronic properties of *Al* and *Ag* nano-porous ultrathin layers in terms of the arrangement and size of the pores were studied. Compared to the highly disordered nano-porous layers, ordered ones exhibit a slightly higher transmittance in the wavelength range of the plasmonic response (up to 10%). However, the ordered nano-porous layers show a drastic increment of the sheet resistance up to 12 times. The use of the ordered nano-porous layers offers great advantage if the sheet resistance is an important concern for applications. The ordered/random *Ag* nano-porous layers having the strong plasmonic response over whole visible range can reach the average transmittance of 90/80% at the sheet resistance of 10/20 Ohm/sq, which is comparable to widely used ITO electrode.

Acknowledgment

Financial support of National Research Foundation of Singapore (NRF7-CRP6-2010-2 and NRF-CRP12-2013-04).